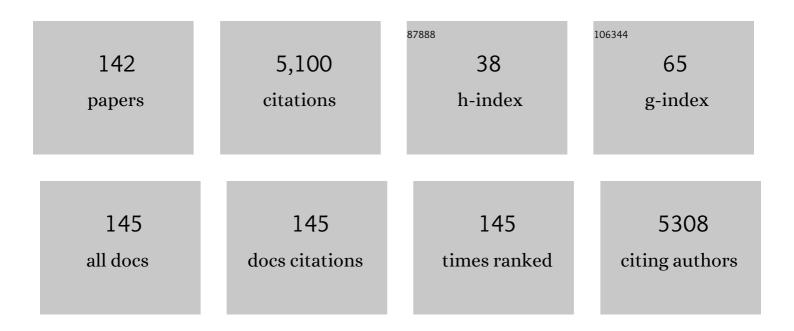
Brandon Q Mercado

List of Publications by Year in descending order

Source: https://exaly.com/author-pdf/3324721/publications.pdf Version: 2024-02-01



#	Article	IF	CITATIONS
1	Iron Complexes of a Proton-Responsive SCS Pincer Ligand with a Sensitive Electronic Structure. Inorganic Chemistry, 2022, 61, 1644-1658.	4.0	7
2	Spin States, Bonding and Magnetism in Mixedâ€Valence Iron(0)â€Iron(II) Complexes**. Chemistry - A European Journal, 2022, 28, .	3.3	4
3	Ligand and solvent effects on CO ₂ insertion into group 10 metal alkyl bonds. Chemical Science, 2022, 13, 2391-2404.	7.4	9
4	Structural and Thermodynamic Effects on the Kinetics of C–H Oxidation by Multisite Proton-Coupled Electron Transfer in Fluorenyl Benzoates. Journal of Organic Chemistry, 2022, , .	3.2	3
5	Control of Catalyst Isomers Using an <i>N</i> -Phenyl-Substituted RN(CH ₂ CH ₂ P ⁱ Pr ₂) ₂ Pincer Ligand in CO ₂ Hydrogenation and Formic Acid Dehydrogenation. Inorganic Chemistry, 2022, 61, 643-656.	4.0	13
6	Facile conversion of ammonia to a nitride in a rhenium system that cleaves dinitrogen. Chemical Science, 2022, 13, 4010-4018.	7.4	11
7	Stereoselective Synthesis of Allenyl Alcohols by Cobalt(III)â€Catalyzed Sequential Câ^'H Bond Addition to 1,3â€Enynes and Aldehydes. Angewandte Chemie, 2022, 134, .	2.0	2
8	Stereoselective Synthesis of Allenyl Alcohols by Cobalt(III) atalyzed Sequential Câ^'H Bond Addition to 1,3â€Enynes and Aldehydes. Angewandte Chemie - International Edition, 2022, 61, .	13.8	10
9	Electrocatalytic, Homogeneous Ammonia Oxidation in Water to Nitrate and Nitrite with a Copper Complex. Journal of the American Chemical Society, 2022, 144, 8449-8453.	13.7	31
10	Synthesis and Reactivity of Iron Complexes with a Biomimetic SCS Pincer Ligand. Inorganic Chemistry, 2021, 60, 1965-1974.	4.0	13
11	Three-Component 1,2-Carboamidation of Bridged Bicyclic Alkenes via Rh ^{III} -Catalyzed Addition of C–H Bonds and Amidating Reagents. Organic Letters, 2021, 23, 2836-2840.	4.6	38
12	All Four Atropisomers of Iron Tetra(<i>o</i> - <i>N</i> , <i>N</i> , <i>N</i> -trimethylanilinium)porphyrin in Both the Ferric and Ferrous States. Inorganic Chemistry, 2021, 60, 5240-5251.	4.0	14
13	Electronic and Spin-State Effects on Dinitrogen Splitting to Nitrides in a Rhenium Pincer System. Inorganic Chemistry, 2021, 60, 6115-6124.	4.0	12
14	Small Molecule Microcrystal Electron Diffraction for the Pharmaceutical Industry–Lessons Learned From Examining Over Fifty Samples. Frontiers in Molecular Biosciences, 2021, 8, 648603.	3.5	27
15	Understanding the Reactivity and Decomposition of a Highly Active Iron Pincer Catalyst for Hydrogenation and Dehydrogenation Reactions. ACS Catalysis, 2021, 11, 10631-10646.	11.2	11
16	Dehydrogenative Synthesis of Carbamates from Formamides and Alcohols Using a Pincer-Supported Iron Catalyst. ACS Catalysis, 2021, 11, 10614-10624.	11.2	7
17	Distorted Copper(II) Complex with Unusually Short CF···Cu Distances. Inorganic Chemistry, 2021, 60, 14759-14764.	4.0	1
18	Accessing Molecular Dimeric Ir Water Oxidation Catalysts from Coordination Precursors. Inorganic Chemistry, 2021, 60, 14349-14356.	4.0	12

#	Article	IF	CITATIONS
19	Chirality-matched catalyst-controlled macrocyclization reactions. Proceedings of the National Academy of Sciences of the United States of America, 2021, 118, .	7.1	9
20	Tunable and Practical Homogeneous Organic Reductants for Cross-Electrophile Coupling. Journal of the American Chemical Society, 2021, 143, 21024-21036.	13.7	23
21	Cobalt(III)-Catalyzed Diastereoselective Three-Component C–H Bond Addition to Butadiene and Activated Ketones. Synthesis, 2020, 52, 1239-1246.	2.3	11
22	Synthesis of organometallic pincer-supported cobalt(II) complexes. Polyhedron, 2020, 177, 114308.	2.2	3
23	Concerted proton-electron transfer oxidation of phenols and hydrocarbons by a high-valent nickel complex. Chemical Science, 2020, 11, 1683-1690.	7.4	14
24	Intramolecular Electrostatic Effects on O ₂ , CO ₂ , and Acetate Binding to a Cationic Iron Porphyrin. Inorganic Chemistry, 2020, 59, 17402-17414.	4.0	20
25	The influences of carbon donor ligands on biomimetic multi-iron complexes for N ₂ reduction. Chemical Science, 2020, 11, 12710-12720.	7.4	17
26	Coupling dinitrogen and hydrocarbons through aryl migration. Nature, 2020, 584, 221-226.	27.8	75
27	Rh(III)-Catalyzed Imidoyl C–H Carbamylation and Cyclization to Bicyclic [1,3,5]Triazinones. Organic Letters, 2020, 22, 8993-8997.	4.6	7
28	Mechanistic Study of Alkene Hydrosilylation Catalyzed by a β-Dialdiminate Cobalt(I) Complex. Organometallics, 2020, 39, 2415-2424.	2.3	15
29	Development of a Convergent Enantioselective Synthetic Route to (â^)-Myrocin G. Journal of Organic Chemistry, 2020, 85, 8952-8989.	3.2	5
30	Surprisingly big linker-dependence of activity and selectivity in CO ₂ reduction by an iridium(<scp>i</scp>) pincer complex. Chemical Communications, 2020, 56, 9126-9129.	4.1	10
31	Bacterial Autoimmune Drug Metabolism Transforms an Immunomodulator into Structurally and Functionally Divergent Antibiotics. Angewandte Chemie, 2020, 132, 7945-7954.	2.0	3
32	Bacterial Autoimmune Drug Metabolism Transforms an Immunomodulator into Structurally and Functionally Divergent Antibiotics. Angewandte Chemie - International Edition, 2020, 59, 7871-7880.	13.8	12
33	Catalysis-Enabled Access to Cryptic Geldanamycin Oxides. ACS Central Science, 2020, 6, 426-435.	11.3	10
34	Combining scaling relationships overcomes rate versus overpotential trade-offs in O ₂ molecular electrocatalysis. Science Advances, 2020, 6, eaaz3318.	10.3	46
35	Structures of three disubstituted [13]-macrodilactones reveal effects of substitution on macrocycle conformation. Acta Crystallographica Section E: Crystallographic Communications, 2020, 76, 1617-1623.	0.5	0
36	Chemical Oxidation of a Coordinated PNP-Pincer Ligand Forms Unexpected Re–Nitroxide Complexes with Reversal of Nitride Reactivity. Inorganic Chemistry, 2019, 58, 10791-10801.	4.0	19

#	Article	IF	CITATIONS
37	Nitrogenase-Relevant Reactivity of a Synthetic Iron–Sulfur–Carbon Site. Journal of the American Chemical Society, 2019, 141, 13148-13157.	13.7	34
38	Synthesis and Prior Misidentification of 4- <i>tert</i> Butyl-2,6-dinitrobenzaldehyde. Journal of Organic Chemistry, 2019, 84, 12172-12176.	3.2	1
39	Copper(I) SNS pincer complexes: Impact of ligand design and solvent coordination on conformer interconversion from spectroscopic and computational studies. Inorganica Chimica Acta, 2019, 495, 118996.	2.4	6
40	Masked Radicals: Iron Complexes of Trityl, Benzophenone, and Phenylacetylene. Organometallics, 2019, 38, 4224-4232.	2.3	15
41	Planar three-coordinate iron sulfide in a synthetic [4Fe-3S] cluster with biomimetic reactivity. Nature Chemistry, 2019, 11, 1019-1025.	13.6	45
42	Bis(dialkylphosphino)ferrocene-Ligated Nickel(II) Precatalysts for Suzuki–Miyaura Reactions of Aryl Carbonates. Organometallics, 2019, 38, 3377-3387.	2.3	21
43	A [2Fe–1S] Complex That Affords Access to Bimetallic and Higher-Nuclearity Iron–Sulfur Clusters. Inorganic Chemistry, 2019, 58, 8829-8834.	4.0	15
44	Terahertz Spectroscopy of Tetrameric Peptides. Journal of Physical Chemistry Letters, 2019, 10, 2624-2628.	4.6	39
45	Roles of Iron Complexes in Catalytic Radical Alkene Cross-Coupling: A Computational and Mechanistic Study. Journal of the American Chemical Society, 2019, 141, 7473-7485.	13.7	78
46	Synthesis and Reactivity of Paramagnetic Nickel Polypyridyl Complexes Relevant to C(sp ²)–C(sp ³)Coupling Reactions. Angewandte Chemie - International Edition, 2019, 58, 6094-6098.	13.8	76
47	Structure and Reactivity of Highly Twisted <i>N</i> Acylimidazoles. Organic Letters, 2019, 21, 2346-2351.	4.6	11
48	Concerted proton-electron transfer reactions in the Marcus inverted region. Science, 2019, 364, 471-475.	12.6	104
49	Synthesis and Reactivity of Paramagnetic Nickel Polypyridyl Complexes Relevant to C(sp ²)–C(sp ³)Coupling Reactions. Angewandte Chemie, 2019, 131, 6155-6159.	2.0	10
50	Modification of a pyridine-alkoxide ligand during the synthesis of coordination compounds. Inorganica Chimica Acta, 2019, 484, 75-78.	2.4	2
51	Phosphothreonine (pThr)-Based Multifunctional Peptide Catalysis for Asymmetric Baeyer–Villiger Oxidations of Cyclobutanones. ACS Catalysis, 2019, 9, 242-252.	11.2	34
52	Outer-Sphere Control for Divergent Multicatalysis with Common Catalytic Moieties. Journal of Organic Chemistry, 2019, 84, 1664-1672.	3.2	7
53	N,N,O Pincer Ligand with a Deprotonatable Site That Promotes Redoxâ€Leveling, High Mn Oxidation States, and a Mn 2 O 2 Dimer Competent for Catalytic Oxygen Evolution. European Journal of Inorganic Chemistry, 2019, 2019, 2115-2123.	2.0	8
54	Correlative vibrational spectroscopy and 2D X-ray diffraction to probe the mineralization of bone in phosphate-deficient mice. Journal of Applied Crystallography, 2019, 52, 960-971.	4.5	1

#	Article	IF	CITATIONS
55	Selective Conversion of CO2into Isocyanate by Low oordinate Iron Complexes. Angewandte Chemie, 2018, 130, 6617-6621.	2.0	7
56	Reversible Ligandâ€Centered Reduction in Lowâ€Coordinate Iron Formazanate Complexes. Chemistry - A European Journal, 2018, 24, 9417-9425.	3.3	30
57	Selective Conversion of CO 2 into Isocyanate by Low oordinate Iron Complexes. Angewandte Chemie - International Edition, 2018, 57, 6507-6511.	13.8	20
58	Alkali Cation Effects on Redox-Active Formazanate Ligands in Iron Chemistry. Inorganic Chemistry, 2018, 57, 9580-9591.	4.0	30
59	A Dinuclear Iridium(V,V) Oxo-Bridged Complex Characterized Using a Bulk Electrolysis Technique for Crystallizing Highly Oxidizing Compounds. Inorganic Chemistry, 2018, 57, 5684-5691.	4.0	17
60	Formation of Aminocyclopentadienes from Silyldihydropyridines: Ring Contractions Driven by Anion Stabilization. Angewandte Chemie - International Edition, 2018, 57, 6605-6609.	13.8	2
61	Nickel(I) Aryl Species: Synthesis, Properties, and Catalytic Activity. ACS Catalysis, 2018, 8, 2526-2533.	11.2	57
62	Formation of Aminocyclopentadienes from Silyldihydropyridines: Ring Contractions Driven by Anion Stabilization. Angewandte Chemie, 2018, 130, 6715-6719.	2.0	0
63	Rhodium(III)-Catalyzed Imidoyl C–H Activation for Annulations to Azolopyrimidines. Organic Letters, 2018, 20, 2464-2467.	4.6	93
64	Deactivation of a ruthenium(II) N-heterocyclic carbene p-cymene complex during transfer hydrogenation catalysis. Transition Metal Chemistry, 2018, 43, 21-29.	1.4	1
65	A Stereodynamic Redoxâ€Interconversion Network of Vicinal Tertiary and Quaternary Carbon Stereocenters in Hydroquinone–Quinone Hybrid Dihydrobenzofurans. Angewandte Chemie, 2018, 130, 15327-15331.	2.0	3
66	Catalytic Formic Acid Dehydrogenation and CO2 Hydrogenation Using Iron PNRP Pincer Complexes with Isonitrile Ligands. Organometallics, 2018, 37, 3846-3853.	2.3	57
67	Modifications to the Aryl Group of dppf-Ligated Ni σ-Aryl Precatalysts: Impact on Speciation and Catalytic Activity in Suzuki–Miyaura Coupling Reactions. Organometallics, 2018, 37, 3943-3955.	2.3	20
68	A Stereodynamic Redoxâ€Interconversion Network of Vicinal Tertiary and Quaternary Carbon Stereocenters in Hydroquinone–Quinone Hybrid Dihydrobenzofurans. Angewandte Chemie - International Edition, 2018, 57, 15107-15111.	13.8	9
69	Activationless Multiple-Site Concerted Proton–Electron Tunneling. Journal of the American Chemical Society, 2018, 140, 7449-7452.	13.7	24
70	Effects of N ₂ Binding Mode on Iron-Based Functionalization of Dinitrogen to Form an Iron(III) Hydrazido Complex. Journal of the American Chemical Society, 2018, 140, 8586-8598.	13.7	42
71	pH Driven Hydrothermal Syntheses of Neodymium Sulfites and Mixed Sulfate-Sulfites. Crystal Growth and Design, 2018, 18, 5332-5341.	3.0	5
72	Selective and synergistic cobalt(iii)-catalysed three-component C–H bond addition to dienes and aldehydes. Nature Catalysis, 2018, 1, 673-679.	34.4	79

5

#	Article	IF	CITATIONS
73	Water-Nucleophilic Attack Mechanism for the Cu ^{II} (pyalk) ₂ Water-Oxidation Catalyst. ACS Catalysis, 2018, 8, 7952-7960.	11.2	37
74	Iron and Cobalt Diazoalkane Complexes Supported by β-Diketiminate Ligands: A Synthetic, Spectroscopic, and Computational Investigation. Inorganic Chemistry, 2018, 57, 5959-5972.	4.0	15
75	Diazoalkanes in Low-Coordinate Iron Chemistry: Bimetallic Diazoalkyl and Alkylidene Complexes of Iron(II). Inorganic Chemistry, 2017, 56, 1019-1022.	4.0	26
76	Enhancement of Câ^'H Oxidizing Ability in Co–O ₂ â€Complexes through an Isolated Heterobimetallic Oxo Intermediate. Angewandte Chemie - International Edition, 2017, 56, 3211-3215.	13.8	27
77	Rh(III)-Catalyzed Aryl and Alkenyl C–H Bond Addition to Diverse Nitroalkenes. ACS Catalysis, 2017, 7, 150-153.	11.2	116
78	Systematic Study of Effects of Structural Modifications on the Aqueous Solubility of Drug-like Molecules. ACS Medicinal Chemistry Letters, 2017, 8, 124-127.	2.8	31
79	Synthesis of pyridine-alkoxide ligands for formation of polynuclear complexes. New Journal of Chemistry, 2017, 41, 6709-6719.	2.8	12
80	Electrocatalytic Water Oxidation by a Copper(II) Complex of an Oxidation-Resistant Ligand. ACS Catalysis, 2017, 7, 3384-3387.	11.2	149
81	Câ^'H and Câ^'N Activation at Redoxâ€Active Pyridine Complexes of Iron. Angewandte Chemie, 2017, 129, 1089-1092.	2.0	6
82	Diversity of Secondary Structure in Catalytic Peptides with β-Turn-Biased Sequences. Journal of the American Chemical Society, 2017, 139, 492-516.	13.7	101
83	Transfer hydrogenation of ketones catalyzed by complexes of ruthenium(II) with the heterotridentate [P,N,O] ligands (S)-2-[{2-(diphenylphosphanyl)benzylidene}amino]propan-1-ol, (S)-2-[{2-(diphenylphosphanyl)benzyl}amino]propan-1-ol or the [P,N,S] ligand (S)-2-(dimethylamino)-1-(diphenylphosphino)-3-(methylthio)propane. Journal of Organometallic	1.8	7
84	Chemistry, 2017, 850, 74884. Câ"H and Câ"N Activation at Redoxâ€Active Pyridine Complexes of Iron. Angewandte Chemie - International Edition, 2017, 56, 1069-1072.	13.8	20
85	Synthesis and Catalytic Activity of PNP-Supported Iron Complexes with Ancillary Isonitrile Ligands. Organometallics, 2017, 36, 3995-4004.	2.3	27
86	Stereodynamic Quinone–Hydroquinone Molecules That Enantiomerize at sp ³ -Carbon via Redox-Interconversion. Journal of the American Chemical Society, 2017, 139, 15239-15244.	13.7	26
87	Synthesis and Characterization of Iridium(V) Coordination Complexes With an N,Oâ€Donor Organic Ligand. Angewandte Chemie, 2017, 129, 13227-13231.	2.0	11
88	Synthesis and Mechanism of Formation of Hydride–Sulfide Complexes of Iron. Inorganic Chemistry, 2017, 56, 9185-9193.	4.0	7
89	Enhancement of Câ^'H Oxidizing Ability in Co–O ₂ â€Complexes through an Isolated Heterobimetallic Oxo Intermediate. Angewandte Chemie, 2017, 129, 3259-3263.	2.0	22
90	Synthesis and Characterization of Iridium(V) Coordination Complexes With an N,Oâ€Donor Organic Ligand. Angewandte Chemie - International Edition, 2017, 56, 13047-13051.	13.8	24

#	Article	IF	CITATIONS
91	Redox Activity of Oxo-Bridged Iridium Dimers in an N,O-Donor Environment: Characterization of Remarkably Stable Ir(IV,V) Complexes. Journal of the American Chemical Society, 2017, 139, 9672-9683.	13.7	45
92	ENDOR characterization of an iron–alkene complex provides insight into a corresponding organometallic intermediate of nitrogenase. Chemical Science, 2017, 8, 5941-5948.	7.4	8
93	βâ€Alkyloxazolochlorins: Revisiting the Ozonation of Octaalkylporphyrins, and Beyond. Chemistry - A European Journal, 2016, 22, 11706-11718.	3.3	16
94	Stepwise N–H bond formation from N2-derived iron nitride, imide and amide intermediates to ammonia. Chemical Science, 2016, 7, 5736-5746.	7.4	76
95	Catalytic Oxygen Evolution from Manganese Complexes with an Oxidationâ€Resistant N,N,Oâ€Donor Ligand. ChemPlusChem, 2016, 81, 1129-1132.	2.8	18
96	Alkali-Controlled C–H Cleavage or N–C Bond Formation by N ₂ -Derived Iron Nitrides and Imides. Journal of the American Chemical Society, 2016, 138, 11185-11191.	13.7	42
97	Controlling the Conformational Energy of a Phenyl Group by Tuning the Strength of a Nonclassical CH···O Hydrogen Bond: The Case of 5-Phenyl-1,3-dioxane. Journal of Organic Chemistry, 2016, 81, 12116-12127.	3.2	13
98	The tropolone–isobutylamine complex: a hydrogen-bonded troponoid without dominant π–π interactions. Acta Crystallographica Section C, Structural Chemistry, 2016, 72, 730-737.	0.5	0
99	Dinitrogen-Facilitated Reversible Formation of a Si–H Bond in a Pincer-Supported Ni Complex. Organometallics, 2016, 35, 3154-3162.	2.3	33
100	New Regio- and Stereoselective Cascades via Unstabilized Azomethine Ylide Cycloadditions for the Synthesis of Highly Substituted Tropane and Indolizidine Frameworks. Journal of the American Chemical Society, 2016, 138, 12664-12670.	13.7	26
101	Organometallic Iridium Complex Containing a Dianionic, Tridentate, Mixed Organic–Inorganic Ligand. Inorganic Chemistry, 2016, 55, 8121-8129.	4.0	4
102	High Oxidation State Iridium Mono-μ-oxo Dimers Related to Water Oxidation Catalysis. Journal of the American Chemical Society, 2016, 138, 15917-15926.	13.7	41
103	Crystal structure of the thermochromic bis(diethylammonium) tetrachloridocuprate(II) complex. Acta Crystallographica Section E: Crystallographic Communications, 2016, 72, 40-43.	0.5	6
104	Rules of Macrocycle Topology: A [13]â€Macrodilactone Case Study. Chemistry - A European Journal, 2016, 22, 6001-6011.	3.3	9
105	New Ir Bis-Carbonyl Precursor for Water Oxidation Catalysis. Inorganic Chemistry, 2016, 55, 2427-2435.	4.0	28
106	Alkali Metal Variation and Twisting of the FeNNFe Core in Bridging Diiron Dinitrogen Complexes. Inorganic Chemistry, 2016, 55, 2960-2968.	4.0	45
107	Molecular titanium–hydroxamate complexes as models for TiO ₂ surface binding. Chemical Communications, 2016, 52, 2972-2975.	4.1	30
108	Facile solvolysis of a surprisingly twisted tertiary amide. New Journal of Chemistry, 2016, 40, 1974-1981.	2.8	3

#	Article	IF	CITATIONS
109	2â€Aminoethanol Extraction as a Method for Purifying Sc ₃ N@C ₈₀ and for Differentiating Classes of Endohedral Fullerenes on the Basis of Reactivity. Chemistry - A European Journal, 2015, 21, 17035-17043.	3.3	17
110	Synthesis of <i>ent</i> â€Ketorfanol via a C–H Alkenylation/Torquoselective 6ï€ Electrocyclization Cascade. Angewandte Chemie - International Edition, 2015, 54, 12044-12048.	13.8	30
111	Iron catalyzed CO ₂ hydrogenation to formate enhanced by Lewis acid co-catalysts. Chemical Science, 2015, 6, 4291-4299.	7.4	285
112	A Stable Coordination Complex of Rh(IV) in an N,O-Donor Environment. Journal of the American Chemical Society, 2015, 137, 15692-15695.	13.7	27
113	Understanding the Solution and Solid-State Structures of Pd and Pt PSiP Pincer-Supported Hydrides. Inorganic Chemistry, 2015, 54, 11411-11422.	4.0	31
114	Regio- and Diastereoselective Synthesis of Highly Substituted, Oxygenated Piperidines from Tetrahydropyridines. Journal of Organic Chemistry, 2015, 80, 6660-6668.	3.2	25
115	Stereogenic α-carbons determine the shape and topology of [13]-macrodilactones. Organic and Biomolecular Chemistry, 2015, 13, 5086-5089.	2.8	9
116	Effect of Remote Aryl Substituents on the Conformational Equilibria of 2,2-Diaryl-1,3-dioxanes: Importance of Electrostatic Interactions. Journal of Organic Chemistry, 2015, 80, 4108-4115.	3.2	5
117	Oxidized and reduced [2Fe–2S] clusters from an iron(I) synthon. Journal of Biological Inorganic Chemistry, 2015, 20, 875-883.	2.6	21
118	Binding of dinitrogen to an iron–sulfur–carbon site. Nature, 2015, 526, 96-99.	27.8	223
119	Rapid, Regioconvergent, Solvent-Free Alkene Hydrosilylation with a Cobalt Catalyst. Journal of the American Chemical Society, 2015, 137, 13244-13247.	13.7	192
120	Synthesis, Characterization, and Nitrogenase-Relevant Reactions of an Iron Sulfide Complex with a Bridging Hydride. Journal of the American Chemical Society, 2015, 137, 13220-13223.	13.7	25
121	Selective conversion of glycerol to lactic acid with iron pincer precatalysts. Chemical Communications, 2015, 51, 16201-16204.	4.1	86
122	Alkali Metal Control over N–N Cleavage in Iron Complexes. Journal of the American Chemical Society, 2014, 136, 16807-16816.	13.7	103
123	Lewis Acid-Assisted Formic Acid Dehydrogenation Using a Pincer-Supported Iron Catalyst. Journal of the American Chemical Society, 2014, 136, 10234-10237.	13.7	377
124	Distortional Effects of Noncovalent Interactions in the Crystal Lattice of a Cp*Ir(III) Acylhydroxamic Acid Complex: A Joint Experimental–Computational Study. Organometallics, 2014, 33, 4417-4424.	2.3	2
125	Structural insights into [Co4O4(C5H5N)4(CH3CO2)4]+, a rare Co(IV)-containing cuboidal complex. Polyhedron, 2013, 64, 304-307.	2.2	12
126	A single crystal X-ray diffraction study of a fully ordered cocrystal of pristine Sc3N@D3h(5)–C78. Polyhedron, 2013, 58, 129-133.	2.2	7

#	Article	IF	CITATIONS
127	Solution and solid state studies of three new supramolecular compounds of zinc(II), nickel(II) and uranium(VI) with chelidamic acid and 9-aminoacridine. Inorganica Chimica Acta, 2013, 406, 256-265.	2.4	21
128	Ordered Structures from Crystalline Carbon Disulfide Solvates of the Nano-Tubular Fullerenes <i>D</i> _{5h} (1)-C ₉₀ and <i>D</i> _{5h} -C ₇₀ . Crystal Growth and Design, 2013, 13, 4591-4598.	3.0	22
129	Selective Synthesis, Isolation, and Crystallographic Characterization of LaSc ₂ N@ <i>I</i> _{<i>h</i>} -C ₈₀ . Inorganic Chemistry, 2012, 51, 13096-13102.	4.0	45
130	Binary ionic porphyrin nanosheets: electronic and light-harvesting properties regulated by crystal structure. Nanoscale, 2012, 4, 1695.	5.6	49
131	Carbon–Carbon Bond-Forming Reactions of α-Thioaryl Carbonyl Compounds for the Synthesis of Complex Heterocyclic Molecules. Journal of Organic Chemistry, 2012, 77, 160-172. X-ray Crystallographic Characterization of New Soluble Endohedral Fullerenes Utilizing the Popular	3.2	19
132	C ₈₂ Bucky Cage. Isolation and Structural Characterization of Sm@ <i>C</i> _{3<i>v</i>} (7)-C ₈₂ , Sm@ <i>C</i> _{<i>s</i>} (6)-C ₈₂ , and Sm@ <i>C</i> ₂ (5)-C ₈₂ , Journal of the American Chemical Society, 2012, 134,	13.7	57
133	14127-14136. Isolation and Crystallographic Identification of Four Isomers of Sm@C ₉₀ . Journal of the American Chemical Society, 2011, 133, 6299-6306.	13.7	57
134	The Shape of the Sc ₂ (1¼ ₂ -S) Unit Trapped in C ₈₂ : Crystallographic, Computational, and Electrochemical Studies of the Isomers, Sc ₂ (1¼ ₂ -S)@ <i>C</i> _{<i>s</i>} (6)-C ₈₂ and Sc ₂ (1¼ ₂ -S)@ <i>C</i> _{3<i>V</i>} (8)-C ₈₂ . Journal of the	13.7	121
135	American Chemical Society, 2011, 133, 6752-6760. [2 + 2] Cycloaddition Reaction to Sc ₃ N@ <i>I</i> _{<i>h</i>} -C ₈₀ . The Formation of Very Stable [5,6]- and [6,6]-Adducts. Journal of the American Chemical Society, 2011, 133, 1563-1571. Large Endohedral Fullerenes Containing Two Metal Ions,	13.7	85
136	Sm ₂ @ <i>D</i> ₂ (35)-C ₈₈ , Sm ₂ @ <i>C</i> ₁ (21)-C ₉₀ , and Sm ₂ @ <i>D</i> ₃ (85)-C ₉₂ , and Their Relationship to Endohedral Fullerenes Containing Two Gadolinium Ions. Journal of the American Chemical Society, 2011, 133,	13.7	61
137	Very Large, Soluble Endohedral Fullerenes in the Series La ₂ C ₉₀ to La ₂ C ₁₃₈ : Isolation and Crystallographic Characterization of La ₂ @ <i>D</i> ₅ (450)-C ₁₀₀ . Journal of the American Chemical Society, 2011, 133, 15338-15341.	13.7	78
138	Rates of Water Exchange for Two Cobalt(II) Heteropolyoxotungstate Compounds in Aqueous Solution. Chemistry - A European Journal, 2011, 17, 4408-4417.	3.3	52
139	Structural and Electrochemical Property Correlations of Metallic Nitride Endohedral Metallofullerenes. Journal of Physical Chemistry C, 2010, 114, 13003-13009.	3.1	48
140	Sc ₂ (1¼ ₂ -O) Trapped in a Fullerene Cage: The Isolation and Structural Characterization of Sc ₂ (1¼ ₂ -O)@ <i>C</i> _{<i>s</i>} (6)-C ₈₂ and the Relevance of the Thermal and Entropic Effects in Fullerene Isomer Selection. Journal of the American Chemical	13.7	119
141	Society, 2010, 132, 12098-12105. Is the Isolated Pentagon Rule Merely a Suggestion for Endohedral Fullerenes? The Structure of a Second Egg-Shaped Endohedral Fullerene—Gd3N@Cs(39663)-C82. Journal of the American Chemical Society, 2008, 130, 7854-7855.	13.7	129
142	Iron, Cobalt, and Nickel Complexes Supported by a iPrPNPhP Pincer Ligand. Organometallics, 0, , .	2.3	7